available at www.sciencedirect.com

ScienceDirect

journal homepage: www.elsevier.com/locate/compag

Fuzzy logic control of a multispectral imaging sensor for in-field plant sensing

Yunseop Kim[a,*], *John F. Reid*[b,1], *Qin Zhang*[c,2]

[a] *Northern Plains Agricultural Research Laboratory, USDA-ARS, 1500 North Central Avenue, Sidney, MT 59270, USA*
[b] *Moline Technology Innovation Center, John Deere, One John Deere Place, Moline, IL 61265, USA*
[c] *Agricultural and Biological Engineering, University of Illinois at Urbana-Champaign 1304 W. Pennsylvania Avenue, Urbana, IL 61801, USA*

ARTICLE INFO

Article history:
Received 1 December 2006
Received in revised form
6 September 2007
Accepted 10 September 2007

Keywords:
Sensors
Infrared imaging
Cameras
Segmentation
Illumination
Logic

ABSTRACT

The development of an in-field plant sensing system for a site-specific application can protect the environment from excessive chemicals and save management cost while maintaining productivity. A multi-spectral imaging sensor has been introduced and widely used for in-field plant sensing. In order for a robust performance of the spectral imaging sensor under changes in ambient illumination, image quality must be maintained for proper spectral image analysis. Image formation that is affected by camera parameters was identified, and a controller was developed to compensate varying image intensity and to obtain the desired image quality. A fuzzy logic control algorithm was applied to automatically adjust the camera exposure and gain to control image brightness within a targeted gray level. Slow convergence and oscillation were regulated by dynamic membership functions with different weights in each image channel. Images affected by illumination disturbance quickly converged into a desired brightness image within a maximum of five iterations over the entire range of camera gains in all three spectral image channels. An application of in-field plant sensing using the fuzzy logic image controller was evaluated on corn crops for nitrogen detection. The normalized spectral response of the sensor was inversely correlated to a chlorophyll meter with −0.93 and −0.88 in red and green channels, respectively. The development of an image quality controller using fuzzy logic enhanced the reliable performance of the in-field plant sensing system.

© 2007 Elsevier B.V. All rights reserved.

1. Introduction

Plant nutrients and water are essential elements for plant growth. Estimation of plant nutrients and water content gives opportunities to optimize fertilization and irrigation practices by supplying needs site-specifically throughout the growing season. The development of such an in-field plant sensing system will potentially protect the environment from excessive chemicals and save management cost while maintaining productivity.

Spectral sensors to estimate plant health responses have been widely studied for water content (Thomas et al., 1971), plant nutrients (Al-Abbas et al., 1974), leaf senescence (Gausman, 1985), and plant response to nitrogen (Bausch and Duke, 1996; Solie et al., 1996; Borhan and Panigrahi, 1999; Thai et al., 1998; Wilkerson et al., 1999). An image-based spectral

* Corresponding author. Tel.: +1 406 433 9477; fax: +1 406 433 5038.
E-mail addresses: james.kim@ars.usda.gov (Y. Kim), ReidJohnF@JohnDeere.com (J.F. Reid), qinzhang@uiuc.edu (Q. Zhang).
[1] Tel.: +1 309 765 3786; fax: +1 309 765 3807.
[2] Tel.: +1 217 333 9419; fax: +1 217 244 0323.
0168-1699/$ – see front matter © 2007 Elsevier B.V. All rights reserved.
doi:10.1016/j.compag.2007.09.008

sensor has been used to assess spectral signature of plant leaves reflected by solar radiation (Bausch et al., 1998; Kim et al., 2000; Lee et al., 1999) and to take advantage of image processing to eliminate background noises that are major obstacles in spectroscopic measurement addressed by Bausch and Duke (1996).

In-field spectral measurements made under natural ambient illumination are significantly influenced by solar radiation changes from cloudy to sunny, which affects spectral responses at all stages of plant growth. The image histogram obtained by leaf reflectance depends on the intensity and the spectral distribution of the incoming energy. Changes in light energy cause fluctuations in the gray-level distribution of target plants, resulting in an estimation bias. Thus, maintaining the image quality is one of the most critical aspects of in-field spectral measurement for making an appropriate estimate of the plant health response. Appropriate control of camera parameters, such as gain and exposure, has to be made to achieve uniform quality of image brightness.

Many commercial camera systems provide automatic exposure operation, in which the shutter speed or gain is allowed to vary in response to varying illumination conditions. Such internal automatic exposure control optimizes the brightness of the overall image based on a perspective of optimizing the visual appearance to a human observer. Problems occur if used in continuous imaging where image brightness features may vary from scene to scene due to internal camera adjustments (King, 1995).

Fuzzy logic has been applied to exposure control in the camera systems to take advantage of linguistic logic described control systems. Commercial applications of exposure control using fuzzy logic have been shown by Sanyo Electric Co. (Haruki and Kikuchi, 1992) and Sony Video Development Group (Shimizu et al., 1992). Their common objectives were to detect the image condition in the video cameras; such as backlighting and excessive frontlighting in which the luminance of a main object deteriorates, and to compensate exposure in order to obtain the appropriate luminance of the main object.

Haruki and Kikuchi (1992) proposed an approach to weight the luminance data of six sub-areas to put emphasis on the center of the image through exposure control by using fuzzy logic to determine the degree of weighting on each area. Shimizu et al. (1992) used the ratio of the pixels whose luminance was greater than a threshold to total pixels in order to measure the contrast and the area ratio between the target and background. Compensation of exposure as a fuzzy output was obtained from inference rules with two fuzzy inputs. Murakami and Honda (1996) used the color information of hue and chroma of pixels with an input representing the importance of the background. They determined the amount of compensation to control the degree of backlighting and excessive frontlighting using fuzzy reasoning.

These special cases of backlighting and excessive frontlighting are not applicable to plant health sensing, since plants are always under the frontlighting condition from the sunlight as an illumination source when a sensor looks downward (Fig. 1). This study focused on obtaining robust image quality against changes of natural ambient illumination. The objectives of the paper are to develop a control algorithm to compensate for illumination variation and to achieve a consistent image quality using fuzzy logic, and evaluate the performance of the fuzzy logic controller of a multi-spectral image sensor.

2. Methods

2.1. Structure of in-field plant sensing system

An in-field plant sensing system for real-time nitrogen detection using a multi-spectral imaging sensor was the proposed by Kim and Reid (2006). The system consists of a portable computer (PAC 586, Dolch Computer Systems, Inc., Fremont, CA) equipped with a PCI Frame Grabber (FlashBus MV, Integral Technologies, Inc., Indianapolis, IN), a multi-spectral imaging sensor (MSIS), an ambient illumination (AI) sensor (SKR1850A 4-channel, Skye Instruments Ltd., Powys, UK), a GPS, and a vehicle platform (Fig. 1).

The MSIS was a custom-developed 3-CCD camera (Cohu Inc., Poway, CA) with three video channels of green (G) at 550 nm, red (R) at 650 nm, and near-infrared (NIR) at 800 nm with bandwidth of approximately 100 nm for each channel. Images are captured by an image sensor with a resolution of 640 H × 480 V at 8-bit/pixels. A frame grabber (FlashBus MV, Integral Technologies, Inc.) was used to acquire images through a high speed peripheral component interconnect (PCI) interface supporting 24-bit color video with up to 16.8 million colors. FlashBus brings real-time digitized video through the PCI bus directly into system memory (off-screen capture mode) at a video frame rate of 5–15 frames/s or directly into VGA display memory (on-screen capture mode) at a video frame rate of 30 frames/s (Integral Technologies Inc., 1998). A serial interface provided external control of gain and shutter speed for each independent video channel.

The conceptual layout of the spectral imaging system is illustrated in Fig. 2. A plant image is captured by the MSIS and the AI sensor records ambient illumination. The image, affected by AI variation, is compensated for gain and exposure control to centralize the gray-level distribution individually for all three channels (R, G, and NIR). After convergence, the image is segmented to remove non-vegetation components. Finally, an application decision is made based on information given by the system, such as image pixel statistics, AI data, duty cycle of camera exposure, and GPS data (Kim and Reid, 2006). Based on the plant stress level calculated from reflectance estimates, a spray control output is determined and sent to a spray nozzle controller.

For reliable extraction of spectral signatures, each image is acquired such that the gray-level distribution falls within the range of the image digitizer from 0 to 255 for a selected camera setting for gain and exposure control. Changes in ambient illumination in the field require a broad range of camera settings. The camera parameters are dynamically adjusted using a fuzzy logic controller to adjust the camera exposure and gain.

2.2. Image processing

One of the advantages with the use of an image-based spectral sensor is the ability to perform image processing to eliminate

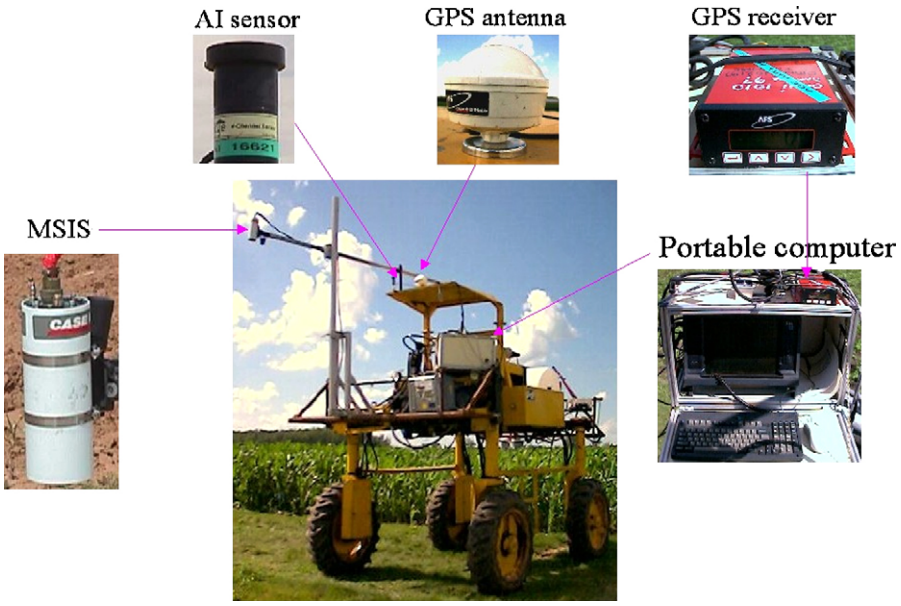

Fig. 1 – Components of the in-field plant sensing system mounted on a sprayer consisting of a multi-spectral imaging sensor (MSIS), an ambient illumination (AI) sensor, a GPS, and a computer.

noisy portions of the sensor response. A target plant image often contains background components such as soil, shadow, and glare pixels. These backgrounds bias leaf reflectance estimates and thus must be eliminated by using image processing.

Segmentation is used to identify object pixels from background pixels. The object pixels of the corn plant canopy portions are obtained by thresholding the image gray-levels for each channel (Fig. 3). Glare portions of leaves and soil are removed by setting a thresholding value of the upper boundary from 255 to 240 in G-channel (Fig. 3(a)) and R-channel (Fig. 3(b), respectively. Shadow and soil backgrounds are eliminated in NIR-channel by changing a thresholding value of the lower boundary from 0 to 66 (Fig. 3(c)) and the upper boundary from 255 to 240 (Fig. 3(d)), respectively. The thresholding values may need adjustment when applying to different types of crop and soil. Further data analysis uses only the segmented portions to derive leaf reflectance measurements and thus it enhances the image to provide a more accurate estimate of plant canopy response. The image is a composite image of three image channels with a non-standard color assignment such that G, NIR, and R channels are displayed as red, green, and blue, respectively.

The threshold values for each image channel are manually selected at the beginning of each data collection session and

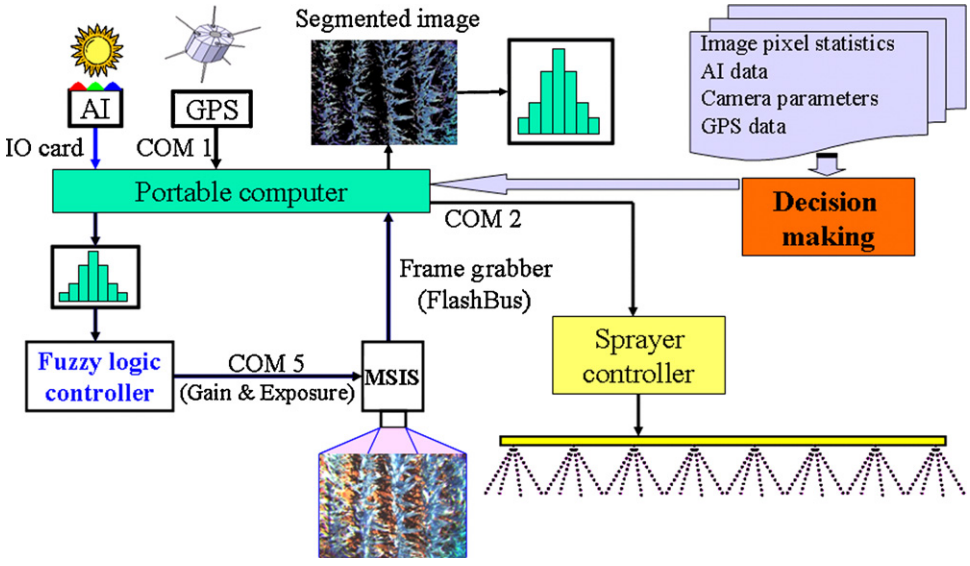

Fig. 2 – Conceptual layout of the spectral imaging system. An image is updated by a fuzzy logic image controller until the image is in optimum brightness, and then segmented for decision making to control the sprayer. RGN stands for red (R), green (G), and near-infrared (N).

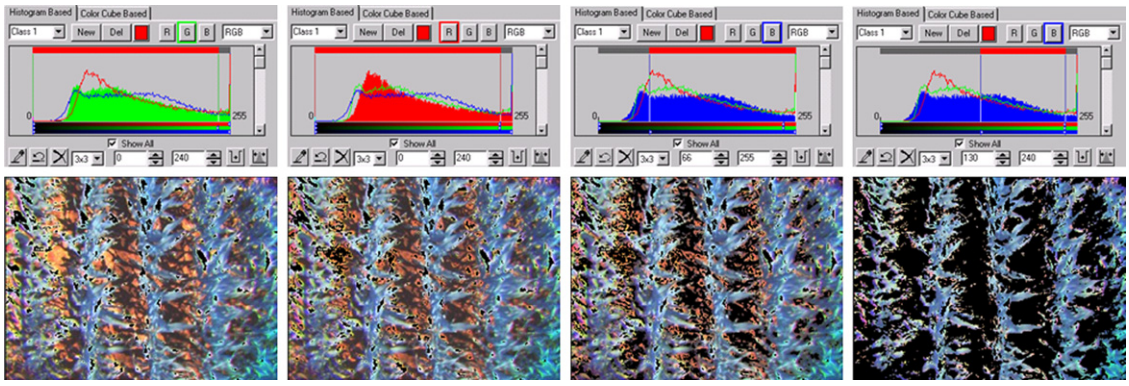

Fig. 3 – Corn plant images into which three image channels were composited: image segmentation to remove (a) glare portions of leaves, (b) glare portions of soil, (c) shadow, and (d) soil.

then fixed for further images collected during that session. Ambient illumination over time may affect the image intensity and thus may sometimes require changing the threshold values. However, a MSIS deploys image acquisition algorithm to capture images at a target brightness achieved by a fuzzy logic controller that dynamically controls the camera parameters. Therefore, the images are always expected to maintain the target image brightness, and the segmentation levels are consistent from image to image.

2.3. *Fuzzy logic controller (FLC)*

Fuzzy logic algorithms have been widely used in many control applications. Unlike a conventional proportional-integral-derivative (PID) controller, the FLC can achieve the goals of steady output and satisfactory transient performance simultaneously (Lee, 1990). However, choices of rule sets and membership functions significantly affect achieving these performance goals (Chen and Hoberock, 1995). Components for the proposed fuzzy logic system are illustrated in Fig. 4. Membership functions are used to transform crisp inputs into fuzzy sets in the process of fuzzification and fuzzy sets back into crisp outputs in the process of defuzzification. The FLC incorporates human knowledge into their knowledge base through fuzzy rules and fuzzy membership functions.

2.3.1. *Fuzzification*

The fuzzy value for input and output is treated as a continuous function, which is called a membership function. A fuzzy set F in a universe of discourse X is characterized by a membership function (μ_F) that takes values within [0,1] and generates a degree of truth.

$$\mu_F : X \rightarrow [0, 1] \tag{1}$$

Fuzzy sets are defined in a continuous mode and represented by triangle membership functions for both input and output. A 50% overlap in the membership functions of all fuzzy sets was used so that only two fuzzy sets had non-zero degree-of-membership functions at any point of the universe of discourse, which reduced the computation. The two degree-of-membership functions (μ_{F1}, μ_{F2}) for input variable (Δx) are defined as:

$$\mu_{F1} = \frac{\Delta x - \text{CrispInput}_1}{\text{CrispInput}_2 - \text{CrispInput}_1}, \tag{2}$$

$$\mu_{F2} = 1 - \mu_{F1}, \tag{3}$$

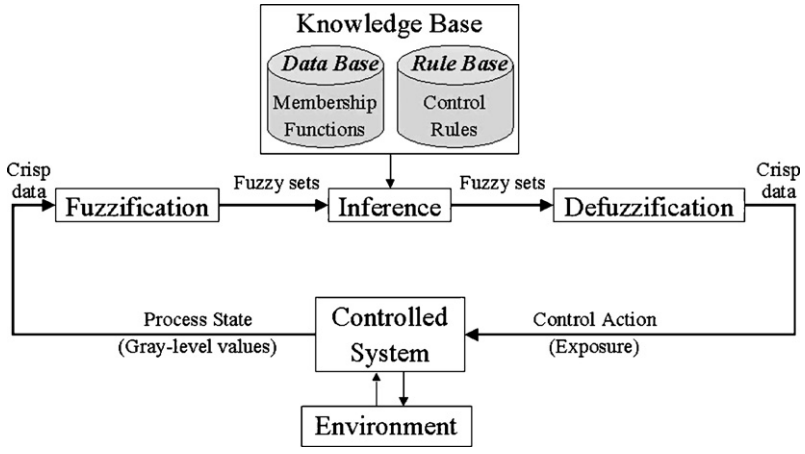

Fig. 4 – Block diagram of fuzzy logic system for image quality control. The fuzzy logic controller optimizes image quality through fuzzy rules and membership functions.

where Δx is the difference of a current image from a target image brightness in an average gray-level (aveGL) scale. CrispInput_1 and CrispInput_2 represent the lower and the upper boundary values, respectively, of two overlapped crisp input domains where the input variable (Δx) is defined.

2.3.2. *Inference rule*

The FLC was designed to have one state input variable and two control output variables. The state input variable (Δx) is the aveGL offset of the current image from a target image with a desired brightness of aveGL = 128, corresponding to the midpoint of the digital number scale from 0 to 255. The control output variables (Δy) are the adjustments of the gain and exposure (ΔGAIN and ΔEXP). Membership domains of input and output are chosen to cover the entire range of possible input and output values, which made scaling unnecessary. The input (Δx) and output (Δy) are partitioned into four membership domains corresponding to four linguistic variables, nil, small, medium, and large. Inference rules that were used in this study are explained as below:

If the error (Δx) is nil, then the adjustment (Δy) is nil.
If the error (Δx) is small, then the adjustment (Δy) is small.
If the error (Δx) is medium, then the adjustment (Δy) is medium.
If the error (Δx) is large, then the adjustment (Δy) is large.

The sign of input variable (Δx) is determined by 128 subtracted by a current aveGL and directly applies to the output: if the input variable is $+\Delta x$ indicating a dark image, the same (+) sign is applied to the output variable (Δy) to increase image brightness, and vice versa.

2.3.3. *Defuzzification*

After obtaining the outputs from the set of fuzzy rules, the rule-based system aggregates the output values and defuzzifies the combined values through the fuzzy inference mechanism for the final decision (Kasabov, 1996). Among many methods applied to the defuzzification stage, the

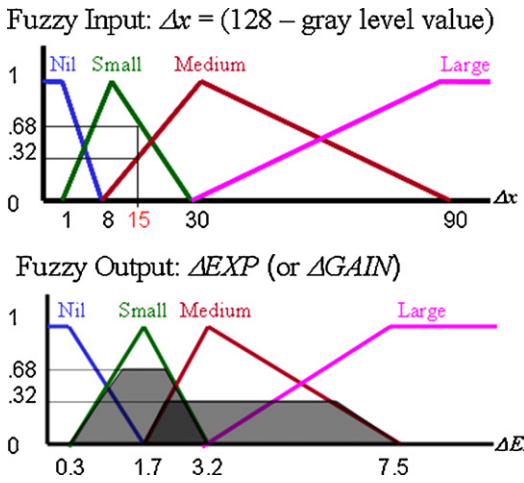

Fig. 5 – Membership functions for fuzzy input (gray-level value difference) and output (exposure or gain). When the input variable is 15, membership functions become 0.32 and 0.68, the output variable is calculated from Eq. (4).

defuzzified compensation value for the control variable (Δy) was defined by:

$$\Delta y = \text{CrispOutput}_2 \times \mu_{F1} + \text{CrispOutput}_1 \times \mu_{F2}, \quad (4)$$

where μ_{F1} and μ_{F2} are two degree-of-membership functions obtained by Eq. (2 and 3), respectively, and CrispOutput_1 and CrispOutput_2 represent the lower and the upper boundary values, respectively, of two overlapped crisp output domains where the output variable (Δy) is defined.

Membership functions for the fuzzy input and output at one of the three channels are illustrated in Fig. 5. If the input variable (Δx) is 15, its membership functions, μ_{F1} and μ_{F2}, are calculated from medium and small, respectively, of the input fuzzy sets (Eqs. (2 and 3)) and the output variable (ΔEXP) is calculated based on corresponding output domains (Eq. (4)) as

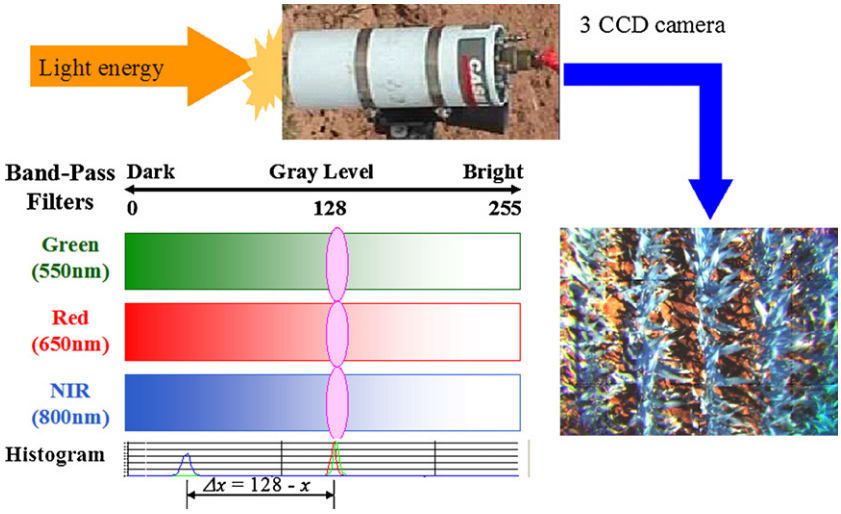

Fig. 6 – Sensor characteristic of a plant sensing system. Each image channel is individually processed to converge to 128. A bottom graph shows image histograms of all three bands where one of them is away and needs to converge to 128.

following:

$$\mu_{F1} = \frac{15-8}{30-8} = 0.32, \quad (5)$$

$$\mu_{F2} = 1 - \mu_{F1} = 0.68, \quad (6)$$

and thus,

$$\Delta\text{EXP} = 3.2 \times \mu_{F1} + 1.7 \times \mu_{F2} = 2.18. \quad (7)$$

2.4. *Image quality control*

The characteristic of the 3-CCD multi-spectral imaging senor for the plant sensing is illustrated in Fig. 6. Light energy coming through the camera generates the image of target plants. Images in each video channel are formatted in a gray-scale from 0 to 255. The image in each channel is individually processed and analyzed. The lower graph of Fig. 6 shows image histograms of all three image bands where one of them is away and needs converge to 128.

A block diagram of the camera control system is shown in Fig. 7. Image brightness in each video channel is determined by both ambient illumination and camera parameter settings. To evaluate the image quality, a mean gray-level value in each channel is compared with a reference value of 128, a middle value of the gray-scale. The resulting difference in each channel is sent to the FLC as fuzzy input to calculate the adjustment of gain and exposure. Gains varies from 0.4 to 4.0 [V] in 16-bit digital representation, while the exposure has 278 stepwise increases ranged from 0 to 100% representing the full open at 1/30 s. Image convergence is obtained by a combination of the two camera parameters.

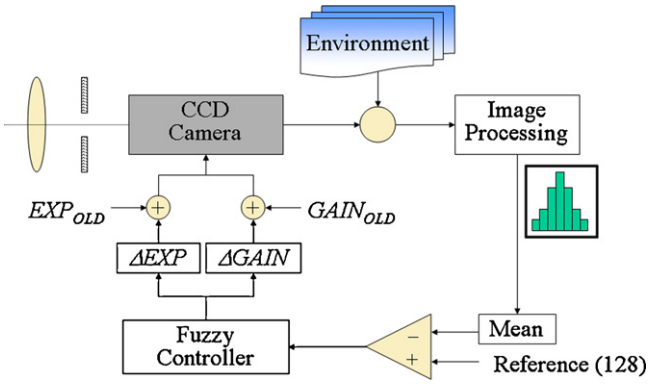

Fig. 7 – Block diagram of the camera control system. Difference of a mean gray-level value from a reference value (128) is used as an input of the fuzzy controller to update the exposure and gain.

3. Experiments and results

3.1. *Image formation of camera parameters: gain and exposure*

An experiment was conducted to find the properties of the camera parameters with respect to reflectance responses. The reflectance of the MSIS was modeled and calibrated with a known reflectance panel perpendicular to the sun (Kim and Reid, 2006). The same setup was used to evaluate the fuzzy logic image controller to minimize bidirectional effects that plant canopies are subject to due to a fixed nadir-view position of the camera under varying solar zenith angles (Kim and Reid, 2007). Two sets of MSISs and AI sensors with a standard 20% reflectance panel (Munsell, GretagMacbeth LLC, New Windsor, NY) was mounted on tripods and oriented coincidently such that all components were perpendicular to the sun, as shown in Fig. 8. Captured images were subject to the shadows of the sensors, but the shadows were removed by image segmentation and only unshaded portions were further processed.

The relationship of gain and exposure is illustrated in Fig. 9. The figure includes the reflectance responses affected by the combination of the gain and exposure. The exposure decreases as the gain increases. Since effects other than the gain changes remained the same, only the exposure had to be reduced to cancel out the magnification effect due to the gain increase.

The resolution of exposure was limited to a minimum value of 0.36% due to the exposure range of 100% divided by stepwise increase of 278. Accordingly, if the exposure increase (ΔExp) generated by the FLC required less than 0.36%, the exposure signal was saturated and thus the response became unstable due to the loss of resolution. This occurred at high gain with low exposure, which generated the loss of consistency in reflectance responses for three channels (Fig. 9). Therefore, it was important to keep the gain as small as possible, which tended to result in higher exposure values. Assuming some boundary effects on the range of the exposure, a value of 80% was selected for a desired value of exposure.

Based on the relationship between gain and exposure, a control algorithm was derived and its flowchart is illustrated in Fig. 10. For each channel, the gain and exposure were initialized with previously used values by reading a file updated every run. Gain control was first performed for coarse tuning to make the error within a gray-level range of ±10, setting

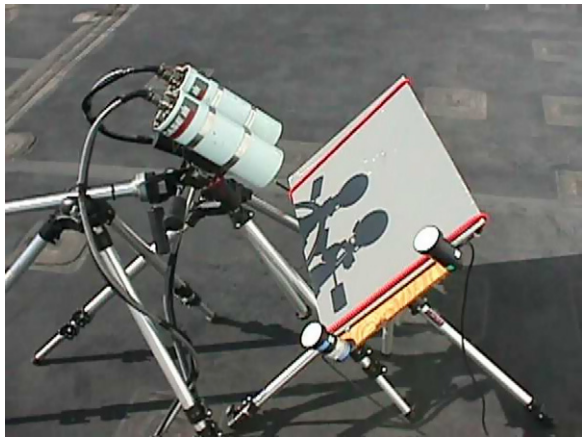

Fig. 8 – Experimental setup of image formation affected by camera parameters. Two sets of MSISs and AI sensors, and a reflectance panel were oriented perpendicular to the sun.

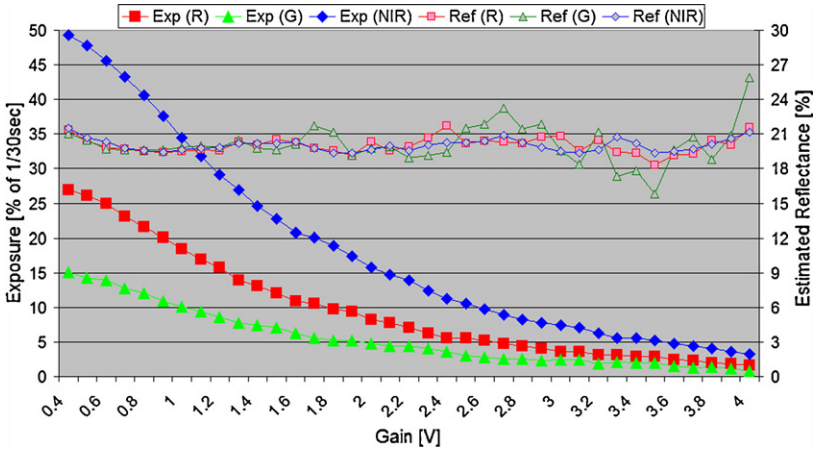

Fig. 9 – MSIS reflectance responses affected by combination of the exposure and gain: stability of the MSIS response decreases as the gain increases.

the exposure to 80%. Then exposure control followed for fine-tuning until the images in all three channels converged to a reference value with a tolerance of ±3 gray-levels. This ensured that the exposure was kept in a high resolution ranging from 50 to 100%. The control loop was terminated if the iteration reached to a maximum of 50 or no adjustment of both gain and exposure in three channels, which happens if saturation conditions occur on a channel.

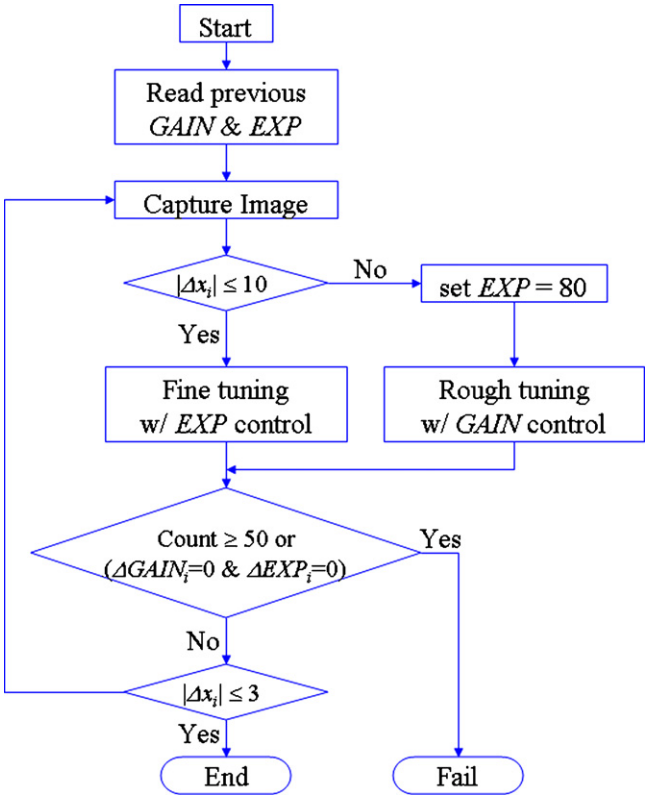

Fig. 10 – Flowchart of image quality control algorithm. Image capture is iterated to update exposure (EXP) and gain (GAIN) until the image deviation (Δx) falls within a tolerance.

3.2. *Fuzzy membership tuning*

A further experiment was performed to evaluate the control algorithm. Membership functions for input and output were chosen for satisfactory image quality by control tuning based on gray-level histograms. Fuzzy sets with fixed membership functions (Fig. 5) were subject to two possible failures: slow convergence and oscillation. Since the gain increased the sensitivity of the exposure adjustment, the slow convergence occurred when the gain was small, while the oscillated response resulted from a high gain. To prevent these problems, membership functions were dynamically adjusted according to the gain.

Another factor to consider was different convergence rate of three channels, because each CCD element had different sensitivity due to optical transfer function differences. In order to prevent the different convergence rate, membership functions were tuned for each channel (i) individually according to its sensitivity by assigning different weight for gain (W_{GAIN}) and exposure (W_{EXP}) as follows:

Fuzzy input domain:

$$\text{Fuzzy Input Domain}\,[0] = 1.0 \tag{8}$$

$$\text{Fuzzy Input Domain}\,[1] = 8.0 + (30.0 - 8.0) \times \frac{(W_{GAINi} - 0.4)}{3.7} \tag{9}$$

$$\text{Fuzzy Input Domain}\,[2] = 30.0 + (90.0 - 30.0) \times \frac{(W_{GAINi} - 0.4)}{3.7} \tag{10}$$

$$\text{Fuzzy Input Domain}\,[3] = 90.0 \tag{11}$$

Fuzzy output domain for gain control:

$$\text{Fuzzy Output Domain}\,[0] = 0.0 \tag{12}$$

$$\text{Fuzzy Output Domain}[1] = 0.05 \times W_{\text{GAINi}} \quad (13)$$

$$\text{Fuzzy Output Domain}[2] = 0.2 \times W_{\text{GAINi}} \quad (14)$$

$$\text{Fuzzy Output Domain}[3] = 0.5 \times W_{\text{GAINi}} \quad (15)$$

Fuzzy output domain for exposure control:

$$\text{Fuzzy Output Domain}[0] = 0.3 \quad (16)$$

$$\text{Fuzzy Output Domain}[1] = 1.7 \times (3.2 - 1.7) \times W_{\text{EXPi}} \times \frac{(4.0 - W_{\text{GAINi}})}{3.6} \quad (17)$$

$$\text{Fuzzy Output Domain}[2] = 3.2 \times (7.5 - 3.2) \times W_{\text{EXPi}} \times \frac{(4.0 - W_{\text{GAINi}})}{3.6} \quad (18)$$

$$\text{Fuzzy Output Domain}[3] = 7.5 \times (10.0 - 7.5) \times W_{\text{EXPi}} \times \frac{(4.0 - W_{\text{GAINi}})}{3.6} \quad (19)$$

3.3. *Image convergence*

The performance of the fuzzy logic image controller was experimentally evaluated using manually selected disturbance. Such condition was artificially created by manually initializing gains and exposures. For example, initializing gain and exposure to a high initial value, an initial image becomes very bright, which was the same situation as the moment of a change from a cloudy to sunny condition.

Accordingly, the experiment was implemented by setting the exposure to a middle value of 50% and varying the gain over a full range from 0.5 [V] to 4.0 [V] with 0.5 [V] increase at each test. With each test set of gains and exposures, the image histograms in all three channels were recorded throughout a control loop to observe the convergence performance individually.

The results of image convergence at R, G, and NIR channels are shown in Figs. 11–13, respectively. In both spectral sensors, images in all three channels quickly converged to a desired range of 128 ± 3 gray-levels for each channel. Most of the images converged within five iterations. Exception to this was saturation in R and G channels that was caused by sensor optical limitation. With approximate 20 Hz processing rate for image control loop, converged images were obtained within a second.

3.4. *In-field plant sensing*

The MSIS system (Fig. 1) associated with image control software was evaluated to detect the crop response relative to nitrogen (N) application treatment and chlorophyll meter (SPAD 502, Minolta Co., Japan). A corn crop was planted on two plots in early and late February. Each plot had 16 rows spaced 76.2 cm apart and of length 105 m. Plots were established by applying eight-stepped treatment of N to create

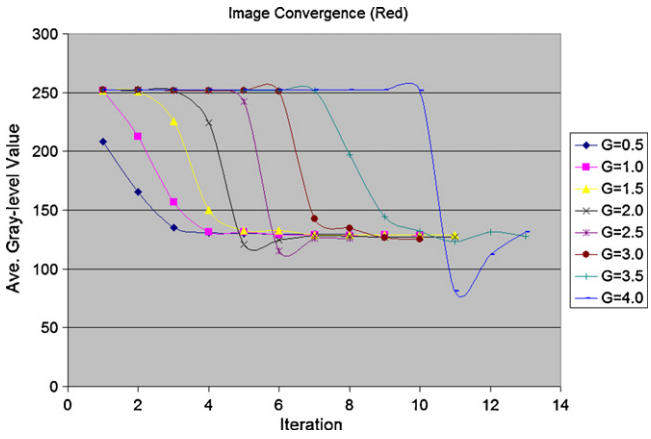

Fig. 11 – Image convergence in red image channel over a full range of the gain. The image starts from saturation (255) at high gains and converges to 128 by the fuzzy logic image controller.

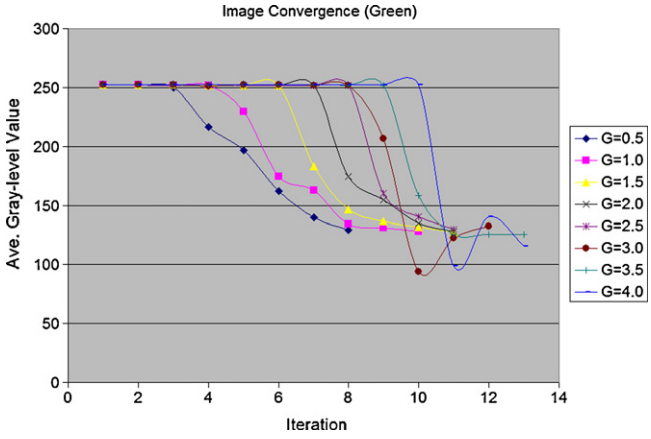

Fig. 12 – Image convergence in green image channel over a full range of the gain. The image starts from saturation (255) at high gains and converges to 128 by the fuzzy logic image controller.

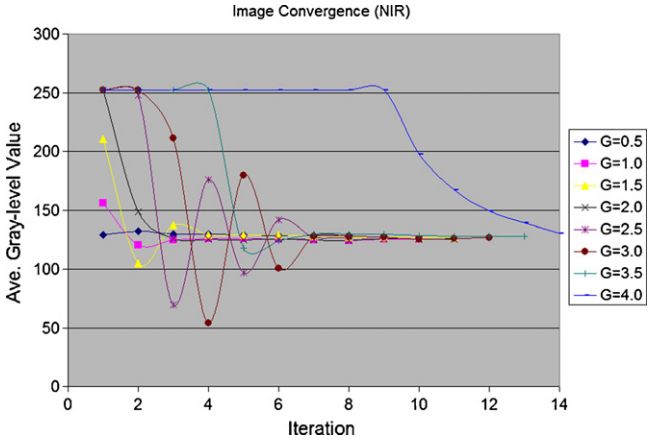

Fig. 13 – Image convergence in NIR image channel over a full range of the gain. The image starts from saturation (255) at high gains and converges to 128 by the fuzzy logic image controller.

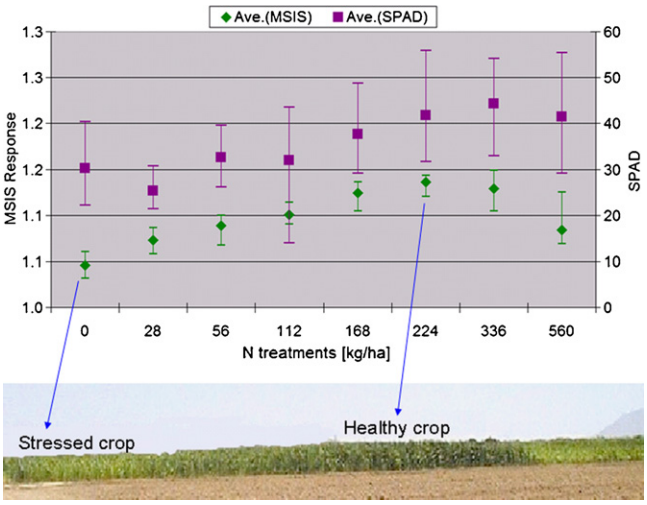

Fig. 14 – MSIS responses compared with SPAD measurements and N treatments on corn crops. Both follow the stepwise-stressed field pattern. The MSIS responses show less variation than SPAD measurements.

differences in crop stress. The SPAD readings ranged from 19 to 24 for severely stressed plants to 45 to 53 for non-stressed plants. Fig. 14 shows comparisons between normalized MSIS responses and SPAD measurements along with variable N treatments. The normalized MSIS response was calculated to estimate N deficiency as a ratio of NDVI to 0.73 as a reference NDVI of healthy crops. Correlation coefficients between the MSIS responses and SPAD measurements were −0.88 and −0.93 in R and G channels, respectively. Both responses closely followed the variation of N treatments. The MSIS response showed a stable distribution, while the SPAD measurements had more variation (Fig. 14). Since the SPAD meter measured only a small area of 2 mm × 3 mm on the plant leaf, the measurements at each location were insufficient to represent the crop field characteristics over the wider area captured by the MSIS.

The fuzzy logic image controller enhanced image acquisitions in optimum brightness and delivered stable response in N assessment of corn plants. Evaluations of the MSIS system with fuzzy logic image controller were further tested on wheat N mapping (Kim et al., 2002), turf glass disease detection (Fermanian et al., 2003), and apple yield mapping (Kim and Reid, 2004).

4. Conclusions

A fuzzy logic controller for an image-based plant sensing system was developed and evaluated to compromise varying ambient illumination. Since a spectral image response was affected by the combinations of gain and exposure, the optimal selection of a combination of gain and exposure was carefully selected by observing the properties of the camera parameters in response to reflectance responses. When the exposure increase required less than the minimum resolution with a high gain, the response became unstable due to the loss of resolution. To minimize the resolution limitation of the exposure, it was desired for the exposure to remain high and for the gain to be as low as possible.

A control algorithm was developed to compensate for illumination variation and maintain image quality using fuzzy logic. The controller adjusted image sensor parameters in response to image feedback. Images affected by ambient illumination converged into a desired image within processing time of less than a second. The simple algorithm used in this study to calculate the degree of membership helped to increase computing speed. Slow convergence and oscillation were regulated by dynamic membership functions with different weights in each channel. An application of plant nitrogen sensing using the multi-spectral imaging sensor with the fuzzy logic image controller presented superior performance of the sensor to a chlorophyll meter. Further applications of the spectral image controller can be extended on different crops to estimate various spectral signatures.

Acknowledgements

The material presented in this paper was based upon work supported partially by CaseIH and USDA Hatch Funds (ILLU-10-352 AE). Any opinions, findings, and conclusions expressed in this publication are those of the authors and do not necessarily reflect the views of the University of Illinois, CaseIH and USDA.

REFERENCES

Al-Abbas, A.H., Barr, R., Hall, J.D., Crane, F.L., Baumgardner, M.F., 1974. Spectra of normal and nutrient-deficient maize leaves. Agron. J. 66 (1), 16–20.

Bausch, W.C., Diker, K., Goetz, A.F.H., Curtis, B., 1998. Hyperspectral characteristics of Nitrogen deficient corn. Agron. J. 66, 16–20.

Bausch, W.C., Duke, H.R., 1996. Remote sensing of plant nitrogen status in corn. Trans. ASABE 39 (5), 1869–1875.

Borhan M.S., S.Panigrahi. 1999. Multi-spectral imaging techniques for nitrogen determination in potato leaf. ASABE paper No. 99-5005. ASABE St. Joseph, MI. 1999.

Chen, B., Hoberock, L.L., 1995. Fuzzy logic controller for automatic vision parameter adjustment in a robotic dish handling system. In: Proceedings of the 1995 IEEE International Symposium on Intelligent Control 38, pp. 332–337.

Fermanian, T., Schmidt, M., Narra, S., Anderson, Z., 2003. Automating the task of evaluating your turf. On Course 57 (1), 21–27, June 2003.

Gausman, H.W., 1985. Plant Leaf Optical Properties. Texas Tech Press, Lubbock, TX.

Haruki, T., Kikuchi, K., 1992. Video camera system using fuzzy logic. IEEE Trans. Cons. Electr. 38, 624–643.

Integral Technologies, Inc. 1998. FlashBus Software Developers Kit. Version 3.2, Indianapolis, IN.

Kasabov, N.K., 1996. Foundations of Neural Networks, Fuzzy Systems, and Knowledge Engineering. The MIT Press, Cambridge, MA.

Kim, Y., Reid, J.F., 2007. Bidirectional effect on a spectral image sensor for in-field crop reflectance assessment. Int. J. Remote Sens. 28 (21), 4913–4926.

Kim, Y., Reid, J.F., 2006. Modeling and calibration of a multi-spectral imaging sensor for in-field crop nitrogen assessment. Appl. Eng. Agric. 22 (6), 935–941.

Kim, Y., Reid, J.F., 2004. Apple yield mapping using a multi-spectral imaging sensor. In: International Conference on Agricultural Engineering, AgEng2004 Paper No. 010-PA-235, Leuven, Belgium.

Kim, Y., Reid, J.F., Huber, G., Schächtl, J., 2002. Real-time nitrogen assessment for wheat using multi-spectral imaging sensor. In: International Conference on Agricultural Engineering, AgEng2002 Paper No. 02-PA-018, Budapest, Hungary, pp. 144–145.

Kim Y., Reid J.F., Hansen A., Dickson M., 2000. Evaluation of a multi-spectral imaging system to detect nitrogen stress of corn crops. ASABE paper No. 00-3128. ASABE, St. Joseph, MI.

King, D.J., 1995. Airborne multispectral digital camera and video sensors: a critical review of system designs and applications. Can. J. Remote Sens. 21 (3), 245–273 (Special issue on aerial optical remote sensing).

Lee, C.C., 1990. Fuzzy logic in control systems: fuzzy logic controller, part I and part II. IEEE Trans. Syst., Man, Cybern. 20 (2), 404–435.

Lee W., Searcy S., Kataoka T. 1999. Assessing nitrogen stress in corn varieties of varying color. ASABE paper No. 99-3034. ASABE, St. Joseph, MI.

Murakami, M., Honda, N., 1996. An exposure control system of video cameras based on fuzzy logic using color information. In: Proceedings of the Fifth IEEE International Conference on Fuzzy Systems, 3, pp. 2181–2187.

Shimizu, S., Kondo, T., Kohashi, T., Tsuruta, M., Komura, T., 1992. A new algorithm control based on fuzzy logic for video cameras. IEEE Trans. Consum. Electr. 38, 617–623.

Solie, J.B., Raun, W.R., Whitney, R.W., Stone, M.L., Ringer, J.D., 1996. Optical sensor based field element size and sensing strategy for nitrogen application. Trans. ASABE 39 (6), 1983–1992.

Thai C.N., Evans M.D., Deng X., Theisen A.F. 1998. Visible & NIR imaging of bush beans grown under different nitrogen treatments. ASABE Paper No. 98-3074. ASABE, St. Joseph, MI.

Thomas, J.R., Namken, L.N., Oerther, G.F., Brown, R.G., 1971. Estimating leaf water content by reflectance measurement. Agron. J. 63, 845–847.

Wilkerson J.B., Sui R., Hart W.E., Wilhelm L.R., Howard D.D. 1999. Artificial neural networks for determining nitrogen status in cotton. ASABE Paper No. 99-3042. ASABE St. Joseph, MI.